1521-0103/12/3402-463–472$25.00
THE JOURNAL OF PHARMACOLOGY AND EXPERIMENTAL THERAPEUTICS
JPET 340:463–472, 2012

Vol. 340, No. 2
187104/3745749

Roscovitine Inhibits $Ca_V3.1$ (T-Type) Channels by Preferentially Affecting Closed-State Inactivation[S]

Viktor Yarotskyy and Keith S. Elmslie

Department of Anesthesiology, Penn State College of Medicine, Hershey, Pennsylvania (V.Y., K.S.E.); and Department of Pharmacology, Kirksville College of Osteopathic Medicine, A.T. Still University, Kirksville, Missouri (K.S.E.)

Received August 18, 2011; accepted November 15, 2011

ABSTRACT

T-type calcium channels (Ca_V3) play an important role in many physiological and pathological processes, including cancerogenesis. Ca_V3 channel blockers have been proposed as potential cancer treatments. Roscovitine, a trisubstituted purine, is a cyclin-dependent kinase (CDK) inhibitor that is currently undergoing phase II clinical trials as an anticancer drug and has been shown to affect calcium and potassium channel activity. Here, we investigate the effect of roscovitine on $Ca_V3.1$ channels. $Ca_V3.1$ channels were transiently expressed in human embryonic kidney 293 cells, and currents were recorded by using the whole-cell patch-clamp technique. Roscovitine blocks $Ca_V3.1$ channels with higher affinity for depolarized cells (EC_{50} of 10 μM), which is associated with a negative shift in the voltage dependence of closed-state inactivation. Enhanced inactivation is mediated by roscovitine-induced acceleration of closed-state inactivation and slowed recovery from inactivation. Small effects of roscovitine were also observed on T-channel deactivation and open-state inactivation, but neither could explain the inhibitory effect. Roscovitine inhibits $Ca_V3.1$ channels within the therapeutic range (10–50 μM) in part by stabilizing the closed-inactivated state. The ability of roscovitine to block multiple mediators of proliferation, including CDKs and $Ca_V3.1$ channels, may facilitate its anticancer properties.

Introduction

T-type calcium channels (Ca_V3) are low voltage-activated channels with fast-inactivation and slow-deactivation kinetics that consist of three family members $Ca_V3.1$ (α_{1G}), $Ca_V3.2$ (α_{1H}), and $Ca_V3.3$ (α_{1I}) (Perez-Reyes, 2003). Ca_V3 channels are widely distributed among different cell types including neurons, cardiomyocytes, and smooth and skeletal muscles (Perez-Reyes, 2003). In spite of establishing many aspects of function and cell specificity, nicely reviewed by Edward Perez-Reyes (Perez-Reyes, 2003), their role in many physiological and pathophysiological processes remains unclear. However, an emerging body of evidence suggests that Ca_V3 channels can participate in pathological processes such as chronic pain (Jagodic et al., 2008) and cancer cell proliferation (Gray and Macdonald, 2006; Lee et al., 2006; Heo et al., 2008; Lu et al., 2008; Taylor et al., 2008a,b). These findings, in particular regarding the channels' role in cancer, have made Ca_V3 channels an attractive clinical target (Gray and Macdonald, 2006).

Roscovitine is a trisubstituted purine, which initially was proposed as an anticancer therapy because of its blocking effect on cyclin-dependent kinases (CDKs) (Meijer et al., 1997; Fischer and Gianella-Borradori, 2003; Wesierska-Gadek et al., 2007). This drug is also known as CYC202 and seliciclib and is currently undergoing phase II clinical trials as a treatment for non–small-cell lung cancer and nasopharyngeal cancer. Emerging evidence suggests that roscovitine may have additional targets involved with tumor development. For example, we have shown that roscovitine can also inhibit human ether-a-go-go related gene (HERG) potassium channel activity (Ganapathi et al., 2009), and HERG channel block can reduce the growth of certain cancer types (Pardo et al., 2005). Ca_V3 channels are potential targets for anticancer therapy (Gray and Macdonald, 2006). $Ca_V3.1$ channels are expressed in many human cancer cell types including liver,

This work was supported in part by grants from the Pennsylvania Department of Health using Tobacco Settlement Funds; and the National Institutes of Health National Institute of Arthritis and Musculoskeletal and Skin Diseases [Grant AR059397].

Article, publication date, and citation information can be found at http://jpet.aspetjournals.org.

http://dx.doi.org/10.1124/jpet.111.187104.

[S] The online version of this article (available at http://jpet.aspetjournals.org) contains supplemental material.

ABBREVIATIONS: CDK, cyclin-dependent kinase; AP, action potential wave form; Cntl, control; DMEM, Dulbecco's modified Eagle's medium; HEK, human embryonic kidney; HERG, human ether-a-go-go related gene; HP, holding potential; I_{SS}, steady-state current; I_{Tail}, tail current amplitude; NMG, *N*-methyl-D-glucamine; Rosc, *R*-roscovitine; τ_{Act}, activation time constant; τ_{CSI}, closed-state inactivation time constant; τ_{Deact}, deactivation time constant; τ_{fast}, fast component recovery from inactivation time constant; τ_{Inact}, inactivation time constant; τ_{slow}, slow component recovery from inactivation time constant; $V_{0.5}$, half-maximal voltage; WO, washout.

ovarian, and breast cancers, and proliferation is reduced by inhibition of these channels by either down-regulation (short interfering RNA) or drug application (Lu et al., 2008; Taylor et al., 2008a; Li et al., 2009, 2011). Through its unique effects on ion channels, roscovitine has provided critical insights into gating mechanisms and the treatment of disease (Buraei et al., 2005, 2007; Cho and Meriney, 2006; Yarotskyy and Elmslie, 2007; Buraei and Elmslie, 2008; Ganapathi et al., 2009; Yarotskyy et al., 2009; Yazawa et al., 2011), which motivated us to test the effect of roscovitine on $Ca_V3.1$ channels. We find that $Ca_V3.1$ channels are inhibited by roscovitine. This inhibition is potentiated by depolarized voltages so that at a membrane potential of −70 mV the EC_{50} is 10 μM, which is at the low end of the therapeutic range (10–50 μM) for roscovitine block of cancer cell proliferation (Meijer et al., 1997; Fischer and Gianella-Borradori, 2003; Wesierska-Gadek et al., 2007). We conclude that the inhibition of $Ca_V3.1$ channels could provide a third anticancer mechanism for roscovitine in addition to CDK and HERG block, which will probably enhance the therapeutic efficacy of roscovitine as an anticancer drug.

Materials and Methods

HEK Cell Transfection. We used either calcium phosphate precipitation (Yarotskyy and Elmslie, 2007) or Lipofectamine 2000 (Yarotskyy et al., 2010) to transfect HEK293 cells with $Ca_V3.1$ channels (cloned from rat pancreatic β cells, a generous gift from Dr. Ming Li, Tulane University Medical School, New Orleans, LA; Genbank no. AF125161) (Zhuang et al., 2000), which provided highly reproducible expression 24 to 48 h after transfection. HEK293 cells were maintained in standard Dulbecco's modified Eagle's medium (DMEM) containing 10% fetal bovine serum and 1% antibiotic-antimycotic mixtures at 37°C in a 5% CO_2 incubator. HEK293 cells were transfected by adding cDNA plasmids as follows: 11.5 μg of α_{1G} ($Ca_V3.1$), 2.15 μg of simian virus 40 large T-antigen (to increase expression efficiency), and 1 μg of green fluorescent protein (to visualize transfected cells). They were incubated at 5% CO_2 for 8 h after which the transfecting medium was replaced by the standard DMEM. The transfected cells were split the next day into 35-mm dishes that served as the recording chamber. Recordings were performed 24 to 48 h after transfection.

Measurement of Ionic Currents. Cells were voltage-clamped by using the whole-cell configuration of the patch-clamp technique. Pipettes were pulled from Schott 8250 glass (Garner Glass, Claremont, CA) on a Sutter P-97 puller (Sutter Instrument Company, Novato, CA). Currents were recorded by using an Axopatch 200A amplifier (Molecular Devices, Sunnyvale, CA) and digitized with an ITC-18 data acquisition interface (Instrutech Corporation, Port Washington, NY). Experiments were controlled by a Power Macintosh G3 computer (Apple Computer, Cupertino, CA) running S5 data acquisition software written by Dr. Stephen Ikeda (National Institutes of Health, National Institute on Alcohol Abuse and Alcoholism, Bethesda, MD). Leak current was subtracted online by using a −P/4 protocol. Recordings were carried out at room temperature, and the holding potential (HP) was −120 mV, unless otherwise stated. Some studies examined $Ca_V3.1$ current activated by an action potential wave form (AP) that was generated by using a series of voltage steps and ramps with the following values (HP = −120 mV): −80 mV for 1 ms, −80 to 37 mV in 0.5 ms, 37 to 40 mV in 0.1 ms, 40 to 37 mV in 0.1 ms, 37 to −80 mV in 1.5 ms, and −80 mV at 11.5 ms. A 20-Hz 10-AP train was generated by using the same voltage changes except that the 1-ms step to −80 mV was removed and voltage between APs within the train was −120 mV. Whole-cell currents were digitized depending on voltage step duration at 50 kHz (up to 100 ms), 10 kHz (200 ms), and 4 kHz (2000 ms) after analog filtering at 1 to 10 kHz.

Data Analysis. Data were analyzed by using IgorPro versions 5 and 6 (WaveMetrics, Lake Oswego, OR) run on a Macintosh computer. Percentage of inhibition was measured by comparing the steady-state drug effect to the average of current measured before [control (Cntl)] and after full recovery [washout (WO)]. Activation time constant (τ_{Act}) was determined by fitting a single exponential function to the step current after a 0.3-ms delay (Buraei et al., 2007). The effect of roscovitine on T-channel inactivation was measured by using either 100- or 1000-ms inactivating voltage steps followed by a 20-ms test step to −20 mV. The I/I_{max} ratio for the current measured from the test step was plotted against inactivating voltage (either 100- or 1000-ms steps) and fitted by a single Boltzmann equation to yield half-maximal voltage ($V_{0.5}$), slope factor (k), and the magnitude of inactivation. Inactivation time constant (τ_{Inact}) was determined by fitting a single exponential function from peak step current to the end of the step. The development of closed-state inactivation was determined by measuring the effect of increasing duration of voltage steps to −70 mV on a 20-ms step to −20 mV (Serrano et al., 1999) (see Fig. 6A). The recovery from inactivation protocol used a 1000-ms inactivating step to either −20 or −70 mV followed by a 20-ms test step to −20 mV after an increasing recovery time at −120 mV. Group data were calculated as mean ± S.D. A paired t test was used for within-cell comparisons. One-way analysis of variance with Tukey honestly significant difference post hoc test was used to test for differences among three or more independent groups.

Solutions. The internal pipette solution contained 104 mM *N*-methyl-D-glucamine (NMG)-Cl, 14 mM creatine-PO_4, 6 mM $MgCl_2$, 10 mM NMG-HEPES, 5 mM Tris-ATP, 0.3 mM Tris-GTP, and 10 mM NMG-EGTA with osmolarity of 280 mOsM and pH 7.3. The external recording solution contained 30 mM $BaCl_2$, 100 mM NMG-Cl, and 10 mM NMG-HEPES with osmolarity of 300 mOsM and pH 7.3. *R*-roscovitine (Rosc) was prepared as a 50 mM stock solution in dimethyl sulfoxide and stored at −30°C. All external solutions contained the same dimethyl sulfoxide concentration so that the roscovitine concentration was the sole variable when changing solutions. Test solutions were applied from a gravity-fed perfusion system that provided complete solution exchange within 1 to 2 s.

Chemicals. All experiments used Rosc (De Azevedo et al., 1997) from LC Labs (Woburn, MA). DMEM, fetal bovine serum, and 100× antibiotic/antimycotic (penicillin, streptomycin, and amphotericin B) were from Invitrogen (Carlsbad, CA). Other chemicals were obtained from Sigma (St. Louis, MO).

Results

Roscovitine Blocks T-Type Channels. Roscovitine has provided surprising insights into ion channel gating mechanisms and disease treatment (Buraei et al., 2005, 2007; Cho and Meriney, 2006; Yarotskyy and Elmslie, 2007; Buraei and Elmslie, 2008; Ganapathi et al., 2009; Yarotskyy et al., 2009; Yazawa et al., 2011). Thus, we were interested in determining whether T-channels would be affected. $Ca_V3.1$ channels expressed in HEK293 cells were activated by using 15-ms depolarizing steps ranging from −100 to +20 mV, followed by repolarization to −100 mV (Fig. 1). Roscovitine (45 μM) strongly blocked the current in a voltage-independent manner (Fig. 1, A–C). Figure 1C shows no significant difference in the percentage of inhibition across all current-generating voltages, which suggests that open channel block is not a mechanism for inhibition. The activation versus voltage relationship was examined in more detail by plotting tail current amplitude (I_{Tail}) versus step voltage (Fig. 1D), which showed a very small right shift induced by 45 μM roscovitine. Single Boltzmann function fitting yielded $V_{0.5}$ for control = −38.0 ± 4.5 mV, roscovitine = −36.7 ± 4.4 mV, and washout = −37.6 ± 4.6 mV (n = 9) (Fig. 1D) and slope factor (k)

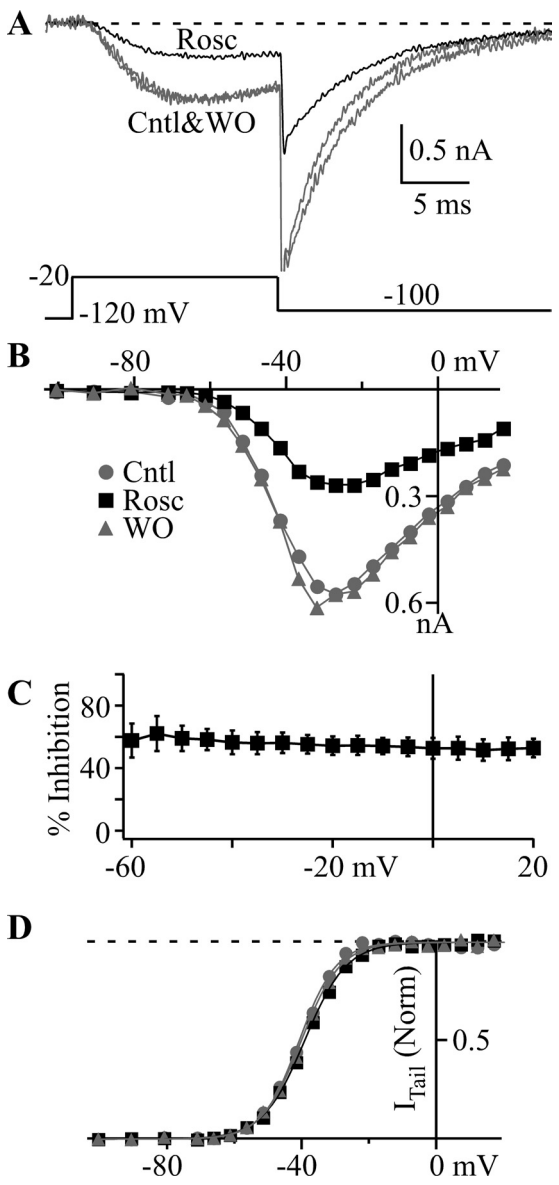

Fig. 1. Roscovitine blocks $Ca_V3.1$ channels. A, typical currents recorded in Cntl (gray), 45 μM Rosc (black), and WO (gray). The voltage protocol is shown below the currents. B, step current versus voltage (*I-V*) relationship from the cell in A demonstrates the inhibitory effect of 45 μM Rosc (black squares) relative to Cntl (gray circles) and WO (gray triangle) across all voltages that evoked current. C, the mean percentage of inhibition (± S.D.; $n = 9$) induced by 45 μM roscovitine was calculated from the average of control and washout currents for voltages that generated current. The flat relationship indicates no voltage dependence of peak current inhibition, which was supported by statistical analysis (analysis of variance) showing no statistical differences across the voltage range. D, normalized I_{Tail} measured 0.3 ms after repolarization to −100 mV is plotted against step voltage for data from the cell in A. Symbols have the same meaning as in B. The smooth lines are single Boltzmann function fits, which yielded $V_{0.5} = -41.0$, −39.4, and −40.4 mV, and slope factor = 5.54, 6.22, and 5.83 for control, 45 μM roscovitine, and washout, respectively. Horizontal dashed line shows maximal open-state occupancy.

of 5.41 ± 0.56, 6.08 ± 0.64, and 6.01 ± 0.82 ($n = 9$) for control, roscovitine, and washout, respectively (Fig. 1D). The roscovitine-induced changes were very small ($\Delta V_{0.5} = 0.9 \pm 0.9$ mV; $\Delta k = 0.38 \pm 0.35$), but significantly different from control ($n = 9$; $p < 0.05$ for both). It is very unlikely that these small changes in activation voltage parameters would have physiological significance.

Roscovitine Does Not Affect Activation but Slows Deactivation of $Ca_V3.1$ Channels. We have reported previously that roscovitine slowed $Ca_V1.2$ channel activation, which contributes to the inhibitory effect (Yarotskyy and Elmslie, 2007; Yarotskyy et al., 2009). For that reason, we examined the effect of roscovitine on $Ca_V3.1$ channel activation speed by comparing τ_{Act} determined by fitting step current onset with a single exponential function. We found no effect of roscovitine on τ_{Act} at any $Ca_V3.1$ current-generating voltage. Indeed, normalized step currents were superimposed in control versus 45 μM roscovitine (Supplemental Fig. 1).

The absence of an effect on $Ca_V3.1$ current activation suggests that the small shift in activation $V_{0.5}$ observed in Fig. 1D is induced by a different mechanism. Because there is precedent for roscovitine to slow calcium channel deactivation (Buraei et al., 2005, 2007), we measured the speed of $Ca_V3.1$ channel closing over voltages ranging from −50 to −160 mV. $Ca_V3.1$ current was activated by 10-ms steps to −10 mV followed by a 72-ms repolarizing (tail) step (Fig. 2). The tail current was fitted by a single exponential function to yield the deactivation time constant (τ_{Deact}), which was plotted against tail voltage (Fig. 2C). Roscovitine significantly increased τ_{Deact} at voltages ranging from −140 to −50 mV ($p < 0.05$). The effect was small and can be better demonstrated by the roscovitine-induced change in τ_{Deact} (% $\Delta\tau_{Deact}$) (Fig. 2D). Qualitatively, this effect is similar to that of roscovitine on $Ca_V2.1$ and $Ca_V2.2$ channels (~7-fold increase in τ_{Deact}) (Buraei et al., 2005, 2007), but the increase of $Ca_V3.1$ current τ_{Deact} was small and did not exceed 20%. This small effect on τ_{Deact} is likely to mediate the minor roscovitine-induced right shift in activation $V_{0.5}$ (Fig. 1D) and could possibly reduce the overall $Ca_V3.1$ current inhibition by a small amount.

Roscovitine Blocks $Ca_V3.1$ Channels in a Dose-Dependent Manner. To determine the dose-dependent effect of roscovitine, we tested the effect of 1, 10, 30, 45, and 100 μM roscovitine on $Ca_V3.1$ current (Fig. 3). Fractional block was plotted against roscovitine concentration and fitted by Hill's equation yielding EC_{50} of 40.5 ± 7.6 μM and Hill's coefficient of 1.55 ± 0.11 ($n = 5$). This EC_{50} was in the range obtained for $Ca_V1.2$ channels (Yarotskyy and Elmslie, 2007). Some Ca_V3 channel blockers, such as mibefradil (McDonough and Bean, 1998), octanol (Eckle and Todorovic, 2010), and T-type antagonist A2 (Uebele et al., 2009), can preferentially affect inactivated channels. We determined whether roscovitine had apparent higher affinity at a more depolarized holding potential at which $Ca_V3.1$ channels inactivate. We found that a −70-mV holding potential significantly decreased the roscovitine EC_{50} of 10.0 ± 1.0 μM, and Hill's coefficient of 1.22 ± 0.15 compared with the results from HP −120 mV (Fig. 3D). This result supports the idea that roscovitine preferentially affects inactivated channels.

Roscovitine Slows Open-State Inactivation. Based on the effect of holding potential on the dose-response relationship, we expected to observe a significant enhancement of inactivation by roscovitine. Using 100-ms voltage steps to inactivate $Ca_V3.1$ channels, we found that roscovitine had the opposite effect with a significant decrease of inactivation at voltages ≥ −40 mV (Fig. 4). There was a small roscovitine-induced enhancement of inactivation, but only at −80 and −70 mV. The more widespread effect was a ~20% decrease of

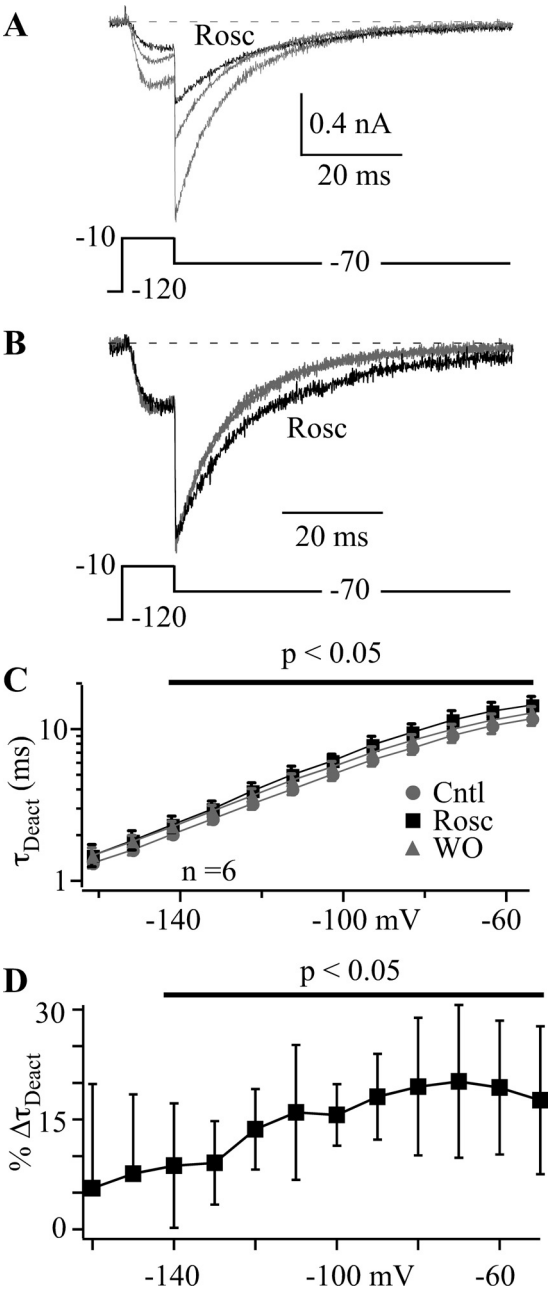

Fig. 2. Roscovitine slowed deactivation of $Ca_V3.1$ channels. A and B, typical currents recorded in control (gray trace), 45 μM Rosc (black trace), and washout (smaller gray trace). The repolarizing step was −70 mV after a depolarizing 10-ms step to −10 mV. The currents in A were normalized to peak tail current (B) to highlight the slower deactivation induced by roscovitine. C, the τ_{Deact} was determined by fitting each tail current with a single exponential function. τ_{Deact} was plotted against repolarizing (tail) voltage to gauge the speed of deactivation over voltages ranging from −50 to −160 mV. Roscovitine significantly increased τ_{Deact} at voltages depolarized to −140 mV (black line; $p < 0.05$; $n = 9$). Data are shown as mean ± S.D. for control (gray circles), 45 μM roscovitine (black squares), and washout (gray triangles). D, the percentage of change in τ_{Deact} ($\%\Delta\tau_{Deact}$) induced by roscovitine (from C) was calculated from the average of control and washout data. The mean ± S.D. are shown with the data significantly different from zero indicated by the line ($p < 0.05$).

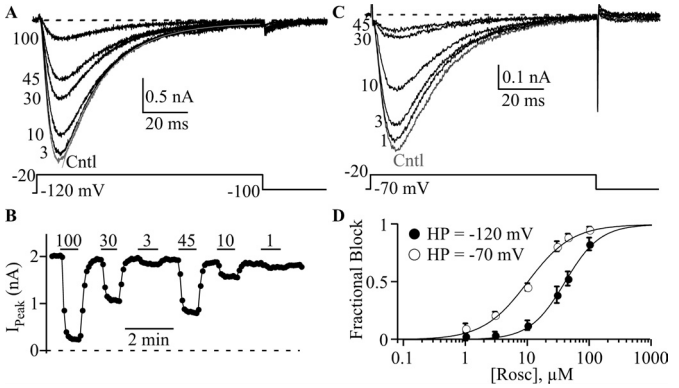

Fig. 3. Roscovitine block is more potent at depolarized holding potentials. A and C, representative traces show the inhibitory effect of roscovitine at −120 mV (A) and −70 mV (C) holding potential. Current was elicited by 100-ms steps to −20 mV from either −120 mV (A) or −70 mV (C). The smooth line on the control current of A is a single exponential fit with τ = 19 ms (see Fig. 4). The numbers at the left of each trace indicate the applied roscovitine concentration (μM). B, the time course for roscovitine inhibition of peak current from the same cell shown in A. The interval between sweeps is 5 s. The horizontal lines indicate the duration of roscovitine application for the given concentration (in μM). D, fractional block is plotted versus roscovitine concentration. Data collected at −120 mV ($n = 5$) and −70 mV ($n = 6$) (HP) are shown as ● and ○, respectively. Smooth lines are Hill's equation fits, which yielded EC_{50} of 40 and 10 μM and Hill's coefficient of 1.53 and 1.21 for HP = −120 and −70 mV, respectively.

inactivation (Fig. 4A) that corresponded with a significant slowing of inactivation at voltages >−40 mV (Fig. 4, B and C). Although decreased inactivation was unexpected, we realized that the reduced inactivation corresponded to current-generating voltages, whereas a small, but significant, enhancement of inactivation was observed at voltages hyperpolarized to channel activation. This suggested that roscovitine may enhance only closed-state inactivation, while slightly decreasing open-state inactivation.

Roscovitine Affects Closed-State Inactivation. The 4-fold reduction in roscovitine EC_{50} with depolarized holding potential (−120 to −70 mV) supports the idea that the inactivated state is stabilized by roscovitine (Fig. 3). Because holding potential changes generally affect closed-state (also called steady-state) inactivation, we tested the effect of longer voltage steps (1000 ms) (Fig. 5), which hyperpolarized the inactivation $V_{0.5}$ by 20 mV from −52 mV for 100 ms to −73 mV for 1000 ms (Fig. 4A versus Fig. 5A) so that much of the inactivation was now observed from closed $Ca_V3.1$ channels. Using this paradigm, 45 μM roscovitine significantly left-shifted the inactivation versus voltage relationship ~10 mV to enhance inactivation at voltages around the resting potential (e.g., −70 mV) (Jones, 1989). Boltzmann equation fits of the inactivation-voltage relationship yielded $V_{0.5} = -73.4 \pm 2.8$, -82.5 ± 2.5, and -72.6 ± 2.8 mV ($n = 6$) for control, roscovitine, and washout, respectively (Fig. 5B). The Boltzmann slope factor was also significantly increased, whereas maximum inactivation was significantly decreased for current generating voltages as observed for inactivation measured from 100-ms steps (Fig. 4A). The enhancement of closed-state inactivation is reminiscent of the inhibitory effect of roscovitine on N-type channels (Buraei and Elmslie, 2008). The decrease in open-state inactivation could have a potentiating effect on $Ca_V3.1$ current, but the enhancement of closed-state inactivation seems to dominate and increase roscovitine-induced inhibition of $Ca_V3.1$ channel activity.

Roscovitine Affects Inactivation Kinetics. The enhancement of closed-state inactivation by roscovitine could result from either an increased speed of inactivation, decreased recovery from inactivation, or both. We examined the time course for the development of closed-state inactivation

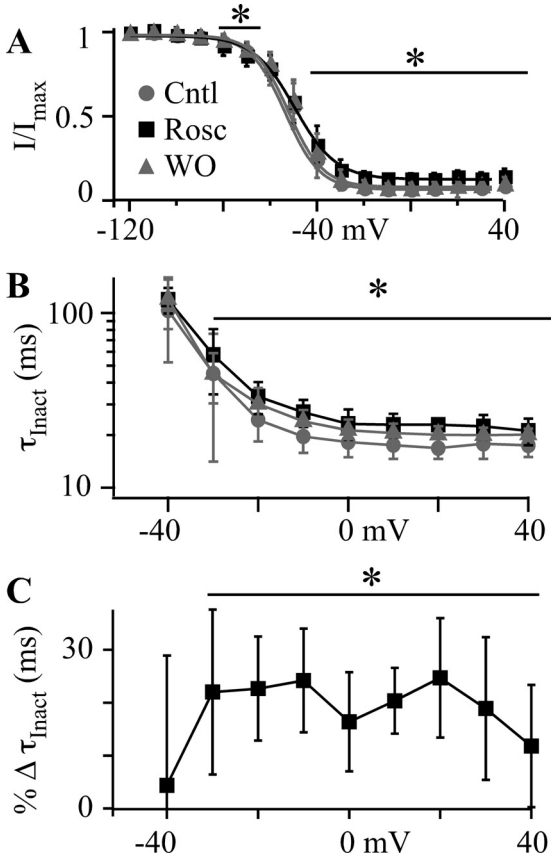

Fig. 4. Roscovitine slows open-state inactivation. A, open-state inactivation was investigated by using a voltage protocol consisting of 100-ms inactivating steps to voltages (V_{Inact}) ranging from −120 to 40 mV followed by 20-ms postpulse to −20 mV to assess channel availability. The postpulse current was normalized to that at −120 mV (I/I_{Max}) and plotted versus V_{Inact} in Cntl (gray circle), 45 μM Rosc (black square), and upon WO (gray triangle) (n = 6). The smooth lines are fits to the inactivation data using the Boltzmann equation, which yielded $V_{0.5}$ = −53.8, −53.7, and −52.6 mV, slope factor = −7.4, −8.7, and −7.4, and maximum inactivation = 0.91, 0.85, and 0.90 for control, 45 μM roscovitine, and washout, respectively. Roscovitine significantly increased inactivation at −80 and −70 mV, but significantly decreased inactivation at voltages ≥−40 mV as indicated by the lines and asterisk ($p < 0.05$). B, the inactivating component of the current was measured by fitting a single exponential equation to current elicited by V_{Inact}. The τ_{Inact} is plotted versus V_{Inact} for control, 45 μM roscovitine, and washout. See Fig. 3A for a representative single exponential fit to inactivation over a 100-ms voltage step. The symbols have the same meaning as in A. τ_{Inact} in roscovitine was significantly larger than control and washout for voltages ≥ −30 mV as indicated by the line and asterisk. C, τ_{Inact} in control and washout was averaged and used to determine the percentage change induced by 45 μM roscovitine (from the data in B). The percentage change in τ_{Inact} (%ΔV_{Inact}) is plotted versus V_{Inact}. The line and asterisk indicate data significantly different from zero ($p < 0.05$).

by examining the effect of increasing the −70-mV step duration (10 to 1900 ms) on current elicited at −20 mV (Fig. 6A). The decrease of $Ca_V3.1$ current with step duration was fitted by single exponential function to yield the closed-state inactivation time constant (τ_{CSI}) at −70 mV (Fig. 6, B and C) and fractional current remaining at the end of the 1900-ms step [steady-state current (I_{SS})] (Fig. 6D). Roscovitine (45 μM) significantly decreased τ_{CSI} by 184 ms (24%; $p < 0.05$; n = 5; Fig. 6C) and I_{SS} by 0.14 (52%; $p < 0.05$; Fig. 6D) relative to the averaged control and washout values (τ_{CSI} = 751 ms; I_{SS} = 0.26). These results show that roscovitine enhances closed-state inactivation by speeding entry into the inactivated state.

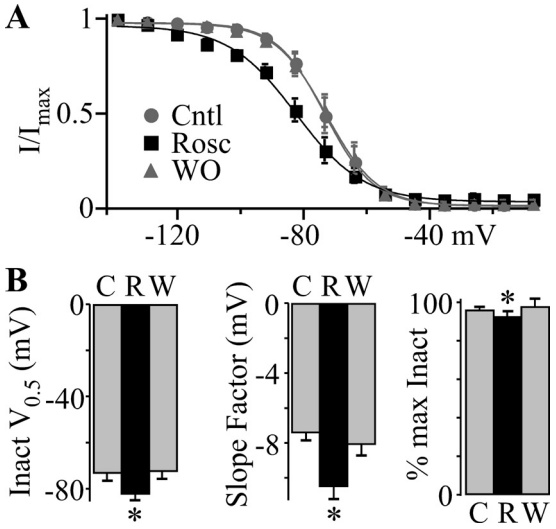

Fig. 5. Roscovitine enhances closed-state inactivation. A, for this study the voltage protocol was similar to that described in Fig. 4 except that the V_{Inact} range was from −140 to 0 mV and the duration was 1000 ms. The postpulse current was normalized to that at −140 mV (I/I_{Max}) and plotted against V_{Inact} for Cntl (gray circles), 45 μM Rosc (black squares), and WO (gray triangles). The smooth lines are single Boltzmann function fits, which yielded $V_{0.5}$ = −73.5, −82.7, and −73.1 mV and slope factor = −7.6, −10.7, and −8.1 for control, roscovitine, and washout, respectively. Roscovitine significantly increased inactivation at voltages from −120 to −40 mV, but significantly decreased inactivation at voltage >−50 mV ($p < 0.05$). B, Boltzmann fitting parameters were averaged from the six cells used to generate A and shows the significant roscovitine-induced decrease in $V_{0.5}$ (left), increase in slope factor (center), and decrease in maximum inactivation (right) (*, $p < 0.05$). Roscovitine data are shown in the black bars (R), and control (C) and washout (W) are shown in gray bars.

The recovery from inactivation was investigated by using 1000-ms inactivating steps (−20 mV) to inactivate $Ca_V3.1$ channels and short test steps to −20 mV of increasing time from the inactivating step to measure the recovery of current (Fig. 7A). The recovery voltage was −120 mV. We found that 45 μM roscovitine significantly slowed recovery from inactivation (Fig. 7, A and B). The recovery time course was best fit by using a double exponential function, which yielded τ_{fast} and τ_{slow} (Fig. 7B). Roscovitine (45 μM) doubled τ_{fast} from 121 ± 36 and 131 ± 21 ms for control and washout, respectively, to 257 ± 89 ms ($p < 0.05$; n = 5), and τ_{slow} was nearly doubled to 1181 ± 227 ms from 652 ± 111 and 695 ± 100 ms (n = 5; $p < 0.05$) in control and washout, respectively. The relative amplitude of the slow recovery component was increased from 56% (average control and washout) to 71% of the total (not significant; p = 0.08). Thus, the enhancement of closed-state inactivation could result from slowed recovery from inactivation as well as faster inactivation. This was further investigated by measuring the recovery from inactivation after 1000-ms steps to −70 mV (Fig. 7C). As observed after −20-mV steps, 45 μM roscovitine significantly slowed the recovery from inactivation generated by −70-mV steps (Fig. 7D). Thus, recovery from closed-state inactivation is slowed by roscovitine. One difference was that the recovery was well described by a single exponential equation with the recovery τ in between the τ_{fast} and τ_{slow} measured after the −20-mV step. The expectation was that the τ values would be similar because the recovery voltage was −120 mV for both data sets. However, it is clear that a slow component of recovery exists after the −70-mV step because the amplitude

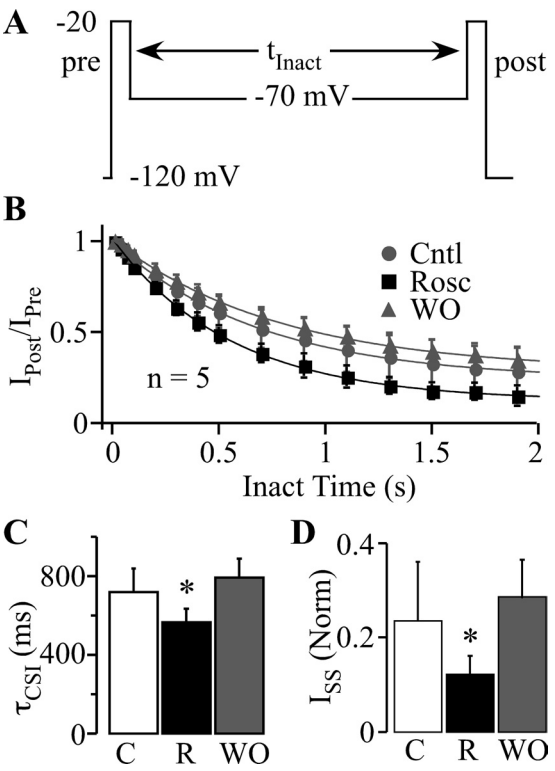

Fig. 6. Roscovitine speeds the development of closed-state inactivation. A, the voltage protocol to investigate the development of inactivation at voltages hyperpolarized to channel activation consisted of two stimuli, prepulse (pre) and postpulse (post), to −20 mV that bracketed a −70-mV step with duration varying from 10 to 1900 ms. B, the postpulse to prepulse current ratio (I_{Post}/I_{Pre}) was plotted against the inactivating step duration, and the data were fitted by single exponential function to yield the time constant of τ_{CSI} and residual I_{SS}. Symbols have the same meaning as in Fig. 5 ($n = 5$). C, roscovitine significantly decreased τ_{CSI} (R; 45 μM), compared with control (C) and WO. D, I_{SS} was significantly decreased in 45 μM roscovitine (R) compared with control (C) and WO ($n = 5$; $p < 0.05$).

of the single exponential function reaches only 93% ($p < 0.05$) of the maximum recovery observed at 15 s (Fig. 7C). The relatively small magnitude of the slow component (7% for −70 mV versus 56% for −20-mV steps) is the likely reason it was not well described by our exponential fitting. Most importantly, our data clearly show that the enhancement of roscovitine-induced inhibition at −70 mV results from accelerated entry into and slowed recovery from closed-state inactivation.

Physiological Impact of Roscovitine. Based on our voltage step data, we speculated that the dominant effect of roscovitine would be inhibition of physiologically activated current. However, deactivation kinetics critically shape Ca^{2+} influx through action potential-activated Ca_V channels (Llinás et al., 1981, 1982; Buraei et al., 2005), and roscovitine significantly slows $Ca_V3.1$ channel deactivation, which could potentially offset inhibition. Thus, we determined the effect of 45 μM roscovitine on $Ca_V3.1$ current activated by a 2-ms AP (Fig. 8). As predicted, roscovitine-induced inhibition dominated with a 53 ± 4% inhibition of charge influx via $Ca_V3.1$ channels (Fig. 8C). Compared with the 53 ± 6% inhibition of step current by 45 μM roscovitine (HP −120 mV; Fig. 3D), it seems that slowed deactivation has little or no effect on the roscovitine-induced inhibition of AP-activated $Ca_V3.1$ current.

A separate issue involves the effect of roscovitine on reducing open-state inactivation. We wanted to determine whether this reduction would have an impact on AP-activated current, which was accomplished by examining the effect of 45 μM roscovitine on $Ca_V3.1$ currents generated during a 10-AP, 20-Hz train (Fig. 9). Under control conditions, $Ca_V3.1$ current decreased with each AP within the train as expected for accumulated inactivation (termed accommodation; Fig. 9, A, B, and D), and roscovitine significantly enhanced accommodation over this 10-AP train (Fig. 9D). As a result, roscovitine-induced inhibition was significantly increased from the first to the 10th AP within the train (Fig. 9, C and E). Thus, the roscovitine-induced reduction of open-state inactivation has little or no effect and is dominated by slowed recovery from inactivation to increase inhibition during the AP train.

Discussion

We have found that roscovitine blocks $Ca_V3.1$ channels in a dose-dependent and holding potential-dependent manner. Depolarizing the holding potential from −120 to −70 mV decreased the EC_{50} by 4-fold. Given that more than 50% of the channels are inactivated at the −70-mV holding potential, we tested the idea that roscovitine enhanced $Ca_V3.1$ channel inactivation. We were surprised to find that inactivation measured from current-generating voltages was slowed by roscovitine to yield a small, but significant, decrease of inactivation. Thus, open-state inactivation was not enhanced by roscovitine. However, longer voltage steps (1000 ms) increased inactivation from closed states, which was significantly enhanced by roscovitine. The development of closed-state inactivation was accelerated by roscovitine, whereas recovery from inactivation was slowed. Thus, increased occupancy of closed-state inactivation is a major mechanism by which roscovitine inhibits T-channel activity.

Roscovitine Inhibits $Ca_V3.1$ Current by Preferentially Affecting Inactivated Channels. We have previously shown that roscovitine-induced inhibition of $Ca_V2.2$ and $Ca_V1.2$ calcium channels was associated with enhanced voltage-dependent inactivation (Yarotskyy and Elmslie, 2007; Buraei and Elmslie, 2008). For $Ca_V2.2$ channels, the roscovitine effect resulted from enhanced closed-state inactivation (Buraei and Elmslie, 2008), whereas $Ca_V1.2$ channel open-state inactivation was selectively affected by roscovitine (Yarotskyy and Elmslie, 2007). Like the $Ca_V2.2$ channel, roscovitine-induced $Ca_V3.1$ channel inhibition was enhanced at depolarized holding potentials that were associated with a 10-mV left shift in the $Ca_V3.1$ channel closed-state inactivation versus voltage relationship. This enhancement results from roscovitine speeding the development of closed-state inactivation and slowing the recovery from inactivation. The acceleration of closed-state inactivation is in stark contrast to the significant slowing of open-state inactivation, which mediated a small, but significant, decrease of open-state inactivation. Thus, roscovitine demonstrates that open- and closed-state inactivation can be differentially modulated in $Ca_V3.1$ channels, which may have clinical benefits. For $Ca_V1.2$ channels, the preferential enhancement of closed-state inactivation by dihydropyridine antagonists (e.g., nifedipine or amlodipine) makes them potent antihypertensive drugs without negative cardiac effects (e.g., negative ionotropy or bradycardia) (Elmslie, 2004).

Our data show that the recovery from inactivation after 1-s

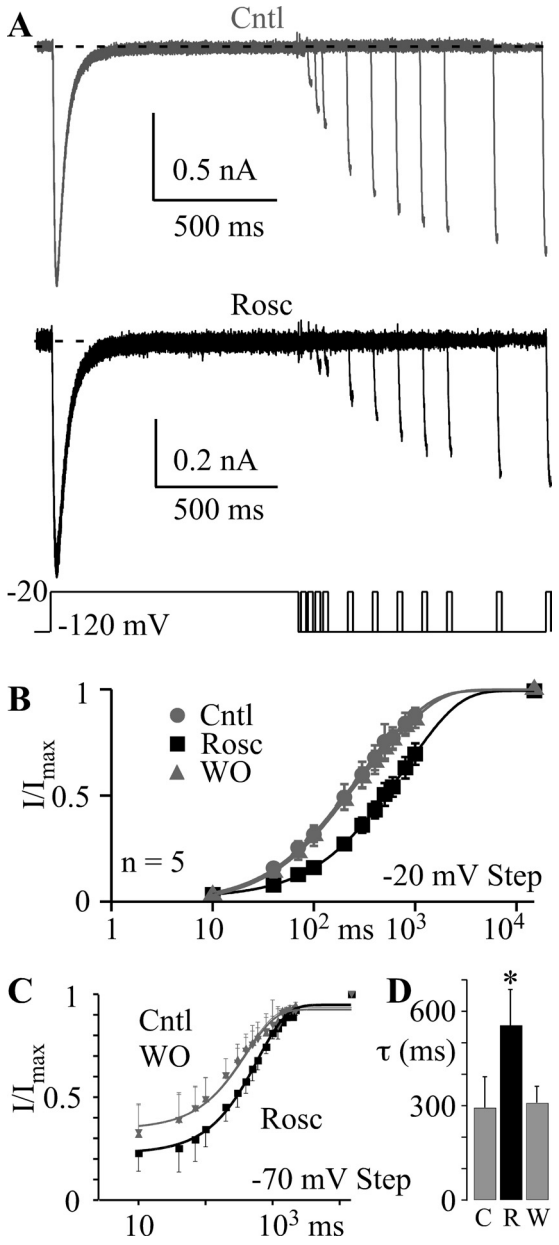

Fig. 7. Roscovitine slows the recovery from inactivation. A, inactivation was induced by a 1000-ms step to −20 mV followed by steps to −120 mV varying from 10 to 1000 ms and a 20-ms postpulse to −20 mV to assess channel availability. Tail currents after the postpulse were removed to more clearly illustrate the recovery from inactivation for control (top) and in 45 μM roscovitine (bottom). B, postpulse currents were normalized to the peak current from the inactivating step and plotted versus recovery time at −120 mV to show the time course for recovery from inactivation for control (gray circles), 45 μM roscovitine (black squares), and washout (gray triangles) ($n = 5$). The 15-s interval between sweeps provided full recovery from inactivation so that was included as the maximum recovery point. The smooth lines are double exponential function fits that yielded τ_{fast} = 118, 246, and 129 ms, and τ_{slow} = 593, 1074, and 691 ms for control, 45 μM roscovitine, and washout, respectively. The amplitude of slow component relative to the fast recovery component (A_{slow}/A_{fast}) was 1.4, 3.3, and 1.3 for control, roscovitine and washout, respectively. C, the recovery from closed-state inactivation was investigated by using a triple pulse protocol where 15-ms steps to −20 mV bracketed a 1000-ms step to −70 mV. For the I/I_{Max} ratio, I_{Max} was measured during the prepulse (before the −70-mV step), and I was measured from the postpulse (after the −70-mV step). The interval between sweeps was 15 s, which provided full recovery from inactivation. The smooth lines are single exponential fits to the data with τ = 402, 609, and 409 ms for control, 45 μM roscovitine and washout, respectively. The fractional amplitude of the recovery component was 0.59, 0.72, and 0.58 for control, roscovitine, and washout, respectively. The recovery at 2200 ms was 95, 92, and 92% of the maximal value (at 15 s) for control, roscovitine, and washout, respectively. D, the recovery τ after 1000-ms steps to −70 mV was averaged from eight cells. The gray bars show control (C) and washout (W) data, and the black bar shows data in 45 μM roscovitine (R). Data are presented as mean ± S.D. (*, $p < 0.05$).

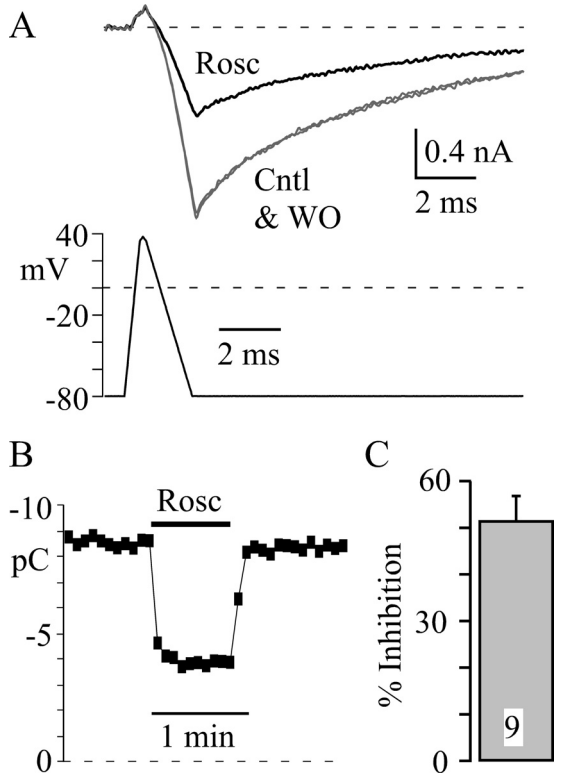

Fig. 8. Roscovitine inhibits physiologically activated $Ca_V3.1$ current. A, $Ca_V3.1$ current was elicited by a 2-ms AP that ranged from −80 to +40 mV. The holding potential was −120 mV, and the voltage was −80 mV for 1 ms before the start of the AP, which was too short to inactivate $Ca_V3.1$ channels. Rosc (45 μM; black trace) inhibited the current relative to that of Cntl and WO (gray trace). B, $Ca_V3.1$ current was integrated from the onset of inward current to the end of the record (12 ms) to determine the charge influx (pC). Roscovitine (45 μM) was applied as indicated by the black bar, and the interval between sweeps was 5 s. C, the mean ± S.D. percentage of inhibition induced by 45 μM roscovitine is shown ($p < 0.05$). The control value for calculating inhibition was the average of current before and upon recovery from roscovitine.

steps to −20 mV was best fit by a double exponential equation in both control and roscovitine supporting multiple components. It is tempting to relate the two recovery components to open-state (fast recovery) and closed-state (slow recovery) inactivation. However, previous work using $Ca_V3.2$ channels demonstrated that recovery was well described by a single exponential process and the time constant was similar if inactivation occurred from either the open or closed state (Serrano et al., 1999), which supports a common recovery pathway for these inactivation processes. Serrano et al. (1999) used short (60 ms) steps to inactivate $Ca_V3.2$ channels from the open state, whereas our step duration was 1 s for studying recovery kinetics. Our measurement of recovery from closed-state inactivation (1 s at −70 mV) clearly had multiple components with the majority of current (93%) recovering by 2.2 s at −120 mV, but full recovery was achieved only within the 15-s interval between sweeps at −120 mV. Unfortunately, this slow component (7%) was too small for an

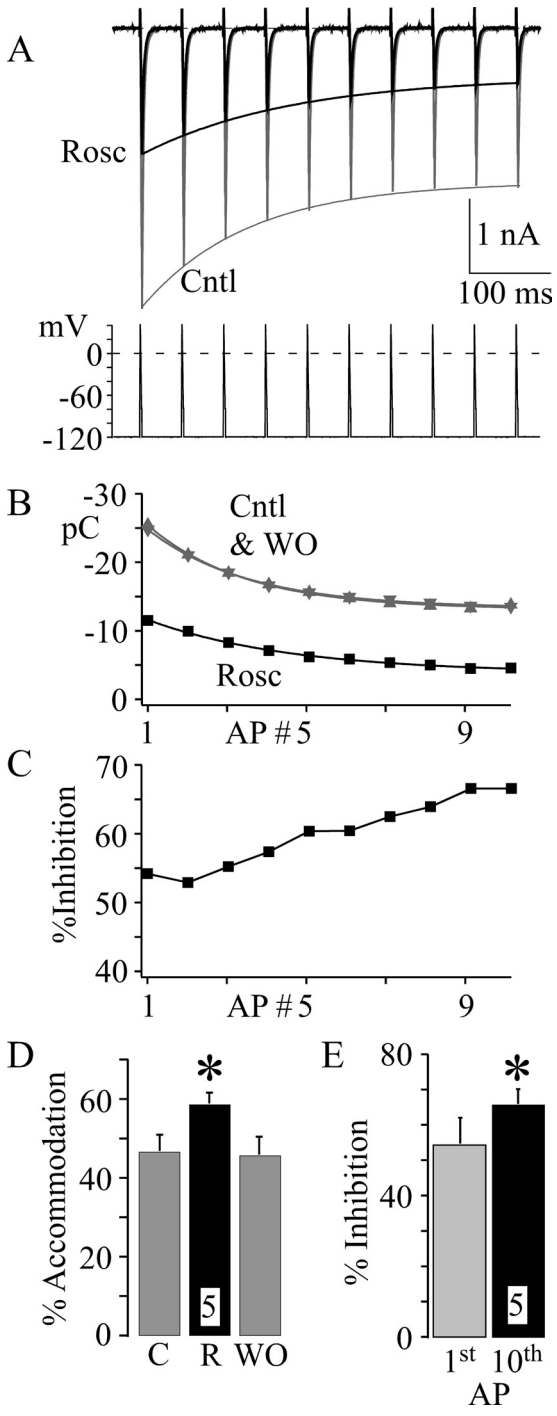

Fig. 9. Increased action potential frequency enhances roscovitine-induced inhibition of $Ca_V3.1$ current. A, currents were generated by a 20-Hz AP train (HP −120 mV) in Cntl (gray trace) and 45 μM Rosc (black trace). For clarity, currents generated upon washout of roscovitine are not shown (but see B). The smooth lines are single exponential fits to the data in B. B, current induced by each AP was integrated over 15 ms and plotted versus the AP number within each train. The smooth lines are single exponential fits to the data. Data are shown in control (gray upward triangle), roscovitine (black square), and upon washout (gray downward triangle) from the same cell in A. C, the roscovitine-induced inhibition was calculated (from B) for each action potential generated current in the train. Note the increase in roscovitine-induced inhibition over the AP train. D, accommodation was calculated as the decrease in current from the first to the last AP in the train. The mean (± S.D.; n = 5) percentage of accommodation is shown for control (C), 45 μM roscovitine (R), and upon recovery (WO). * indicates significant difference from control (average of C and WO; $p < 0.05$). E, the roscovitine-induced inhibition of integrated current was calculated (as in C) for the first and 10th sweep in the action potential train. The average percentage of inhibition (± S.D.; n = 5) induced by 45 μM roscovitine is shown. * indicates that the inhibition of the 10th sweep is significantly ($p < 0.05$) larger than that of the first sweep.

accurate determination of the time course. It has long been recognized that Ca_V3 channels can recover from inactivation with multiple components and the slower recovery component can be increased with longer step durations (Bossu and Feltz, 1986; Herrington and Lingle, 1992). Thus, the slow recovery component may correspond to a slow inactivation state for which occupancy requires longer and stronger depolarization. It is noteworthy that roscovitine significantly slowed recovery to contribute to the enhancement of closed-state inactivation and, thus, inhibition.

One concern was how the multiple effects of roscovitine on $Ca_V3.1$ channels would affect physiologically activated current. Although our data strongly support the dominance of inhibition for $Ca_V3.1$ current activated by voltage steps, deactivation kinetics play an important role in determining Ca^{2+} influx via action potential-activated Ca_V channels (Llinás et al., 1981, 1982; Buraei et al., 2005). Because roscovitine significantly slowed $Ca_V3.1$ channel deactivation, we wanted to determine whether this had a measureable impact. However, there was no difference between the roscovitine-induced inhibition of $Ca_V3.1$ step current versus AP-activated charge influx. Thus, slowed deactivation was probably too small to significantly affect inhibition.

The differential effect of roscovitine on open-state versus closed-state inactivation could also have a physiological impact. Although the decrease of open-state inactivation is small, it is possible that this effect would be measureable under conditions where open-state inactivation dominates. One such condition could be an AP train, where open-state inactivation is expected to accumulate with each pulse. In our test, we used −120 mV as the interpulse potential to limit the potential impact of closed-state inactivation. However, roscovitine still increased inhibition during the AP train so that current during the 10th pulse was significantly smaller than that of the first pulse. This increase is probably the result of the slowed recovery from inactivation induced by roscovitine. Even though open-state inactivation is reduced, the recovery from open-state inactivation at −120 mV is slowed by roscovitine, and it is this slowed recovery that enhances inhibition during the AP train.

Does Closed-State Inactivation Fully Explain Roscovitine-Induced Inhibition? Many T-channel antagonists show enhanced block at depolarized holding potentials, including mibefradil (McDonough and Bean, 1998; Martin et al., 2000), octanol (Eckle and Todorovic, 2010), and T-type antagonist A2 (Uebele et al., 2009). However, significant block of Ca_V3 current at holding potentials that maximally recover Ca_V3 channel inactivation suggests that closed channel block can also occur, but with lower affinity (McDonough and Bean, 1998). This seems to be the case with roscovitine as well. We observed 50% inhibition at −120 mV induced by 45 μM roscovitine. Although this concentration left-shifted the inactivation-voltage relationship 10 mV (1000-ms steps), maximal recovery from inactivation was still achieved at −120 mV (Fig. 5A). Thus, it seems that closed $Ca_V3.1$ channels are sensitive to block by roscovitine,

but this state has at least a 4-fold lower affinity for the drug than the closed inactivation state.

One surprise was that the enhancement of closed-state inactivation by roscovitine is common between $Ca_V2.2$ and $Ca_V3.1$ channels, but open-state inactivation of $Ca_V1.2$ channels is selectively enhanced. Sequence comparisons between the three Ca_V gene families shows much closer homology between the Ca_V1 and Ca_V2 families (~52%) compared with the Ca_V2 and Ca_V3 families (~28%) (Catterall et al., 2005). Based on this, it seems more likely that $Ca_V2.2$ channels would share a common mechanism with $Ca_V1.2$ channels than with $Ca_V3.1$ channels. Roscovitine reveals the potential for similar closed-state inactivation mechanisms between the distantly related $Ca_V2.2$ and $Ca_V3.1$ channels. However, block of closed channels distinguishes $Ca_V3.1$ channel, because no inhibition was observed at holding potentials from which $Ca_V2.2$ channels were fully recovered from closed-state inactivation (Buraei and Elmslie, 2008).

Roscovitine Is a Promising Anticancer Drug that Exhibits Beneficial Polypharmacy. Roscovitine is undergoing phase II clinical trials as an anticancer drug based on its CDK blocking effect (Meijer et al., 1997; Hahntow et al., 2004; Benson et al., 2007; Wesierska-Gadek et al., 2007). Until very recently the anticancer properties were solely linked to CDK block with a therapeutic window of 10 to 50 μM (Meijer et al., 1997; Fischer and Gianella-Borradori, 2003; Hahntow et al., 2004). We showed that roscovitine's anticancer effect may also involve potassium channel blockade (Ganapathi et al., 2009). HERG potassium channels can regulate cancer cell proliferation, and HERG blockers have been shown to reduce proliferation and invasiveness (Arcangeli, 2005; Masi et al., 2005; Pardo et al., 2005; Raschi et al., 2008). Thus, HERG blockers have been proposed as an adjuvant cancer therapy (Pillozzi et al., 2007; Raschi et al., 2008). Roscovitine blocked HERG channels with an EC_{50} of 27 μM, which could complement the CDK inhibition to more potently suppress the cancer cell development. Here, we reveal a third potential anticancer activity of this drug, which is to inhibit calcium entry through $Ca_V3.1$ channels with an EC_{50} of 10 μM at the −70-mV holding potential (at the low end of the roscovitine therapeutic window). Although polypharmacy was once thought to be an undesirable property for a drug, more recent insights have revealed the important benefits of multiple drug actions in treating disease, and polypharmacy has gained new importance in the pharmaceutical industry (Hopkins, 2008; Howitz and Sinclair, 2008; Yang et al., 2008).

Ca_V3 channels seem to support abnormal calcium entry to enhance the proliferation of cancer cells, and Ca_V3 channel blockers are promising anticancer drugs (Gray and Macdonald, 2006; Lee et al., 2006; Heo et al., 2008; Lu et al., 2008; Taylor et al., 2008a,b). Roscovitine more potently blocks $Ca_V3.1$ channels in the closed inactivated state, which increases its affinity at more depolarized holding potentials. Changes in membrane potential that are controlled by potassium channel activity (e.g., HERG) seem to be critical in the control of cell proliferation by enhancing calcium entry and controlling cell volume (Pardo, 2004). Roscovitine block of potassium channel activity would depolarize the cancer cell to increase $Ca_V3.1$ channel closed-state inactivation and enhance roscovitine inhibition of $Ca_V3.1$ channel activity. Thus, the polypharmacy action of roscovitine could have synergistic benefits.

Authorship Contributions

Participated in research design: Yarotskyy and Elmslie.
Conducted experiments: Yarotskyy and Elmslie.
Performed data analysis: Yarotskyy and Elmslie.
Wrote or contributed to the writing of the manuscript: Yarotskyy and Elmslie.

References

Arcangeli A (2005) Expression and role of hERG channels in cancer cells. *Novartis Found Symp* **266:**225–232; discussion 232–234.

Benson C, White J, De Bono J, O'Donnell A, Raynaud F, Cruickshank C, McGrath H, Walton M, Workman P, Kaye S, et al. (2007) A phase I trial of the selective oral cyclin-dependent kinase inhibitor seliciclib (CYC202; *R*-Roscovitine), administered twice daily for 7 days every 21 days. *Br J Cancer* **96:**29–37.

Bossu JL and Feltz A (1986) Inactivation of the low-threshold transient calcium current in rat sensory neurones: evidence for a dual process. *J Physiol* **376:**341–357.

Buraei Z, Anghelescu M, and Elmslie KS (2005) Slowed N-type calcium channel ($Ca_V2.2$) deactivation by the cyclin-dependent kinase inhibitor roscovitine. *Biophys J* **89:**1681–1691.

Buraei Z and Elmslie KS (2008) The separation of antagonist from agonist effects of trisubstituted purines on $Ca_V2.2$ (N-type) channels. *J Neurochem* **105:**1450–1461.

Buraei Z, Schofield G, and Elmslie KS (2007) Roscovitine differentially affects Ca_V2 and K_v channels by binding to the open state. *Neuropharmacology* **52:**883–894.

Catterall WA, Perez-Reyes E, Snutch TP, and Striessnig J (2005) International Union of Pharmacology. XLVIII. Nomenclature and structure-function relationships of voltage-gated calcium channels. *Pharmacol Rev* **57:**411–425.

Cho S and Meriney SD (2006) The effects of presynaptic calcium channel modulation by roscovitine on transmitter release at the adult frog neuromuscular junction. *Eur J Neurosci* **23:**3200–3208.

De Azevedo WF, Leclerc S, Meijer L, Havlicek L, Strnad M, and Kim SH (1997) Inhibition of cyclin-dependent kinases by purine analogues: crystal structure of human cdk2 complexed with roscovitine. *Eur J Biochem* **243:**518–526.

Eckle VS and Todorovic SM (2010) Mechanisms of inhibition of $Ca_V3.1$ T-type calcium current by aliphatic alcohols. *Neuropharmacology* **59:**58–69.

Elmslie KS (2004) Calcium channel blockers in the treatment of disease. *J Neurosci Res* **75:**733–741.

Fischer PM and Gianella-Borradori A (2003) CDK inhibitors in clinical development for the treatment of cancer. *Expert Opin Investig Drugs* **12:**955–970.

Ganapathi SB, Kester M, and Elmslie KS (2009) State-dependent block of HERG potassium channels by R-roscovitine: implications for cancer therapy. *Am J Physiol Cell Physiol* **296:**C701–C710.

Gray LS and Macdonald TL (2006) The pharmacology and regulation of T type calcium channels: new opportunities for unique therapeutics for cancer. *Cell Calcium* **40:**115–120.

Hahntow IN, Schneller F, Oelsner M, Weick K, Ringshausen I, Fend F, Peschel C, and Decker T (2004) Cyclin-dependent kinase inhibitor roscovitine induces apoptosis in chronic lymphocytic leukemia cells. *Leukemia* **18:**747–755.

Heo JH, Seo HN, Choe YJ, Kim S, Oh CR, Kim YD, Rhim H, Choo DJ, Kim J, and Lee JY (2008) T-type Ca^{2+} channel blockers suppress the growth of human cancer cells. *Bioorg Med Chem Lett* **18:**3899–3901.

Herrington J and Lingle CJ (1992) Kinetic and pharmacological properties of low voltage-activated Ca^{2+} current in rat clonal (GH3) pituitary cells. *J Neurophysiol* **68:**213–232.

Hopkins AL (2008) Network pharmacology: the next paradigm in drug discovery. *Nat Chem Biol* **4:**682–690.

Howitz KT and Sinclair DA (2008) Xenohormesis: sensing the chemical cues of other species. *Cell* **133:**387–391.

Jagodic MM, Pathirathna S, Joksovic PM, Lee W, Nelson MT, Naik AK, Su P, Jevtovic-Todorovic V, and Todorovic SM (2008) Up-regulation of the T-type calcium current in small rat sensory neurons after chronic constrictive injury of the sciatic nerve. *J Neurophysiol* **99:**3151–3156.

Jones SW (1989) On the resting potential of isolated frog sympathetic neurons. *Neuron* **3:**153–161.

Lee JY, Park SJ, Park SJ, Lee MJ, Rhim H, Seo SH, and Kim KS (2006) Growth inhibition of human cancer cells in vitro by T-type calcium channel blockers. *Bioorg Med Chem Lett* **16:**5014–5017.

Li W, Zhang SL, Wang N, Zhang BB, and Li M (2011) Blockade of T-type Ca^{2+} channels inhibits human ovarian cancer cell proliferation. *Cancer Invest* **29:**339–346.

Li Y, Liu S, Lu F, Zhang T, Chen H, Wu S, and Zhuang H (2009) A role of functional T-type Ca^{2+} channel in hepatocellular carcinoma cell proliferation. *Oncol Rep* **22:**1229–1235.

Llinás R, Steinberg IZ, and Walton K (1981) Relationship between presynaptic calcium current and postsynaptic potential in squid giant synapse. *Biophys J* **33:**323–351.

Llinás R, Sugimori M, and Simon SM (1982) Transmission by presynaptic spike-like depolarization in the squid giant synapse. *Proc Natl Acad Sci U S A* **79:**2415–2419.

Lu F, Chen H, Zhou C, Liu S, Guo M, Chen P, Zhuang H, Xie D, and Wu S (2008) T-type Ca^{2+} channel expression in human esophageal carcinomas: a functional role in proliferation. *Cell Calcium* **43:**49–58.

Martin RL, Lee JH, Cribbs LL, Perez-Reyes E, and Hanck DA (2000) Mibefradil block of cloned T-type calcium channels. *J Pharmacol Exp Ther* **295:**302–308.

Masi A, Becchetti A, Restano-Cassulini R, Polvani S, Hofmann G, Buccoliero AM, Paglierani M, Pollo B, Taddei GL, Gallina P, et al. (2005) hERG1 channels are overexpressed in glioblastoma multiforme and modulate VEGF secretion in glioblastoma cell lines. *Br J Cancer* **93:**781–792.

McDonough SI and Bean BP (1998) Mibefradil inhibition of T-type calcium channels in cerebellar purkinje neurons. *Mol Pharmacol* **54:**1080–1087.
Meijer L, Borgne A, Mulner O, Chong JP, Blow JJ, Inagaki N, Inagaki M, Delcros JG, and Moulinoux JP (1997) Biochemical and cellular effects of roscovitine, a potent and selective inhibitor of the cyclin-dependent kinases cdc2, cdk2 and cdk5. *Eur J Biochem* **243:**527–536.
Pardo LA (2004) Voltage-gated potassium channels in cell proliferation. *Physiology (Bethesda)* **19:**285–292.
Pardo LA, Contreras-Jurado C, Zientkowska M, Alves F, and Stühmer W (2005) Role of voltage-gated potassium channels in cancer. *J Membr Biol* **205:**115–124.
Perez-Reyes E (2003) Molecular physiology of low-voltage-activated T-type calcium channels. *Physiol Rev* **83:**117–161.
Pillozzi S, Brizzi MF, Bernabei PA, Bartolozzi B, Caporale R, Basile V, Boddi V, Pegoraro L, Becchetti A, and Arcangeli A (2007) VEGFR-1 (FLT-1), β1 integrin, and hERG K^+ channel for a macromolecular signaling complex in acute myeloid leukemia: role in cell migration and clinical outcome. *Blood* **110:**1238–1250.
Raschi E, Vasina V, Poluzzi E, and De Ponti F (2008) The hERG K^+ channel: target and antitarget strategies in drug development. *Pharmacol Res* **57:**181–195.
Serrano JR, Perez-Reyes E, and Jones SW (1999) State-dependent inactivation of the α1G T-type calcium channel. *J Gen Physiol* **114:**185–201.
Taylor JT, Huang L, Pottle JE, Liu K, Yang Y, Zeng X, Keyser BM, Agrawal KC, Hansen JB, and Li M (2008a) Selective blockade of T-type Ca^{2+} channels suppresses human breast cancer cell proliferation. *Cancer Lett* **267:**116–124.
Taylor JT, Zeng XB, Pottle JE, Lee K, Wang AR, Yi SG, Scruggs JA, Sikka SS, and Li M (2008b) Calcium signaling and T-type calcium channels in cancer cell cycling. *World J Gastroenterol* **14:**4984–4991.
Uebele VN, Gotter AL, Nuss CE, Kraus RL, Doran SM, Garson SL, Reiss DR, Li Y, Barrow JC, Reger TS, et al. (2009) Antagonism of T-type calcium channels inhibits high-fat diet-induced weight gain in mice. *J Clin Invest* **119:**1659–1667.
Wesierska-Gadek J, Schmitz ML, and Ranftler C (2007) Roscovitine-activated HIP2 kinase induces phosphorylation of wt p53 at Ser-46 in human MCF-7 breast cancer cells. *J Cell Biochem* **100:**865–874.
Yang K, Bai H, Ouyang Q, Lai L, and Tang C (2008) Finding multiple target optimal intervention in disease-related molecular network. *Mol Syst Biol* **4:**228.
Yarotskyy V and Elmslie KS (2007) Roscovitine, a cyclin-dependent kinase inhibitor, affects several gating mechanisms to inhibit cardiac L-type ($Ca_V1.2$) calcium channels. *Br J Pharmacol* **152:**386–395.
Yarotskyy V, Gao G, Du L, Ganapathi SB, Peterson BZ, and Elmslie KS (2010) Roscovitine binds to novel L-channel ($Ca_V1.2$) sites that separately affect activation and inactivation. *J Biol Chem* **285:**43–53.
Yarotskyy V, Gao G, Peterson BZ, and Elmslie KS (2009) The Timothy syndrome mutation of cardiac $Ca_V1.2$ (L-type) channels: multiple altered gating mechanisms and pharmacological restoration of inactivation. *J Physiol* **587:**551–565.
Yazawa M, Hsueh B, Jia X, Pasca AM, Bernstein JA, Hallmayer J, and Dolmetsch RE (2011) Using induced pluripotent stem cells to investigate cardiac phenotypes in Timothy syndrome. *Nature* **471:**230–234.
Zhuang H, Bhattacharjee A, Hu F, Zhang M, Goswami T, Wang L, Wu S, Berggren PO, and Li M (2000) Cloning of a T-type Ca^{2+} channel isoform in insulin-secreting cells. *Diabetes* **49:**59–64.

Address correspondence to: Viktor Yarotskyy, Department of Pharmacology and Physiology, University of Rochester Medical Center, 601 Elmwood Avenue, Rochester, NY 14642. E-mail: viktor_yarotskyy@urmc.rochester.edu